Epilepsia. Author manuscript; available in PMC 2016 May 19.

Published in final edited form as:
Epilepsia. 2012 March ; 53(3): 459–468. doi:10.1111/j.1528-1167.2012.03408.x.

On the ictogenic properties of the piriform cortex in vitro

Gabriella Panuccio[*,1], **Gonzalo Sanchez**[*,1], **Maxime Lévesque**[*], **Pariya Salami**[*], **Marco de Curtis**[†], and **Massimo Avoli**[*]

[*]Montreal Neurological Institute and Department of Neurology & Neurosurgery, McGill University, Montreal, Quebec, Canada

[†]Unit of Experimental Neurophysiology and Epileptology, Neurological Institute Carlo Besta, Milano, Italy

Summary

Purpose—The piriform cortex (PC) is known to be epileptic-prone and it may be involved in the manifestation of limbic seizures. Herein, we have characterized some electrophysiologic and pharmacologic properties of the spontaneous epileptiform activity generated by PC networks maintained in vitro.

Methods—We performed field potential recordings from the PC in coronal or sagittal rat brain slices along with pharmacologic manipulations of γ-aminobutyric acid (GABA)ergic and glutamatergic signaling during application of the convulsant drug 4-aminopyridine (4AP, 50 μM).

Key Findings—Coronal and sagittal preparations generated interictal-like and ictal-like epileptiform discharges with similar duration and frequency. Ictal-like discharges in sagittal slices were initiated mostly in the PC anterior subregion, whereas interictal activity did not have any preferential site of origin. In sagittal slices, high frequency oscillations (HFOs) at 80–200 Hz were detected mainly at the beginning of the ictal discharge in both posterior and anterior subregions. *N*-Methyl-D-aspartate (NMDA) receptor antagonism abolished ictal discharges, but failed to influence interictal activity. In the absence of ionotropic glutamatergic transmission, PC networks generated slow, GABA receptor–dependent events. Finally, $GABA_A$ receptor antagonism during application of 4AP only, abolished ictal discharges and disclosed recurrent interictal activity.

Significance—Our findings demonstrate that PC networks can sustain in vitro epileptiform activity induced by 4AP. HFOs, which emerge at the onset of ictal activity, may be involved in PC ictogenesis. As reported in several cortical structures, ionotropic glutamatergic neurotransmission is necessary but not sufficient for ictal discharge generation, a process that also requires operative $GABA_A$ receptor–mediated signaling.

Keywords

4-Aminopyridine; Ictogenesis; GABA; Glutamate; High-frequency oscillations

Address correspondence to Massimo Avoli, 3801 University Street, Montreal, QC H3A 2B4, Canada. massimo.avoli@mcgill.ca.
[1]These authors contributed equally to this study.

Disclosure
None of the authors has any conflict of interest to disclose. We confirm that we have read the Journal's position on issues involved in ethical publication and affirm that this report is consistent with those guidelines.

The piriform cortex (PC) is a large cytoarchitectonically homogeneous area that is part of the olfactory region, and it extends in rodents over the ventrolateral surface of the forebrain (Price, 1973; Luskin & Price, 1983). Network activity in the olfactory system is expressed by oscillations in the beta (15–40 Hz) and gamma (50–100 Hz) frequency ranges, the amplitude and frequency of which may reflect experience-driven plasticity (Neville & Haberly, 2003). The PC is indeed a highly seizure-prone region (Piredda & Gale, 1985; Hoffman & Haberly, 1991), and several studies support its involvement in the manifestation of limbic seizures (de Curtis et al., 1994; Loscher & Ebert, 1996; Demir et al., 1998, 1999b, 2001). As extensively reviewed by Shipley and Ennis (1996) and by Haberly (2001), this three-layered cortical area projects to several limbic structures, such as amygdala (Veening, 1978; Wakefield, 1980; Carlsen et al., 1982; Russchen, 1982), lateral entorhinal cortex, and subiculum (Krettek & Price, 1977, 1978). These brain structures are closely involved in limbic seizures that occur in patients with temporal lobe epilepsy (Mathern et al., 1997).

A clear subdivision of the PC has been made between the anterior and posterior subregions with regard to connectivity (Haberly, 2001), and it has been shown that the intrinsic PC inhibitory circuitry has a functional gradient across the rostrocaudal axis in that γ-aminobutyric acid (GABA)ergic inputs are stronger in the posterior subregion (Luna & Pettit, 2010; see also Haberly, 2001; Loscher & Ebert, 1996). The anterior PC would be, therefore, expected to be more susceptible to seizure induction by application of convulsant drugs or electrical kindling, even though some investigators have proposed that only the central PC is crucially involved in epileptogenic processes (McIntyre et al., 2000; Schwabe et al., 2000). In vitro studies have shown that the entire PC is sensitive to seizure induction (Hoffman & Haberly, 1991; de Curtis et al., 1994; Federico et al., 1994; Demir et al., 1999b), whereas in vivo studies have demonstrated that its epileptiform hyperexcitability rather lies within its deep layers (Piredda & Gale, 1985; Ebert et al., 2000). The piriform region has also been proposed to be involved in secondary generalization of seizures in studies performed in rodent models of epilepsy and seizures (Piredda & Gale, 1985; Loscher & Ebert, 1996). This concept was revived recently by a functional magnetic resonance imaging (fMRI) study on patients with epilepsy that highlighted the presence of hemodynamic increases near the frontal PC ipsilateral to the presumed cortical focus (Laufs et al., 2011).

We have recently reported that intraarterial injection of the convulsant drug 4-aminopyridine (4AP) in the in vitro isolated guinea pig brain induces in the PC seizure-like events, set off by fast oscillatory activity, that can propagate to the entorhinal cortex and to other structures of the limbic system (Carriero et al., 2010). Of interest, in this preparation, $GABA_A$ receptor blockers induce interictal spikes but no seizure activity (de Curtis et al., 1994), unless repetitive seizures involving the limbic regions become generated (Librizzi & de Curtis, 2003; Uva et al., 2005). Therefore, these findings suggest that the PC may contribute to ictogenesis by promoting drug-specific (and thus mechanism-specific) patterns. Currently, information about the mechanisms underlying epileptiform synchronization in the PC, studied by means of brain slices, is scattered and it is largely limited to the analysis of interictal events (Hoffman & Haberly, 1993, 1996; Demir et al., 1999b, 2000, 2001; but see Libri et al., 1996; Demir et al., 1999a). Therefore, in the present study we employed an in vitro brain slice preparation to: (1) characterize electrophysiologic and pharmacologic

features of the 4AP-induced epileptiform activity generated by PC networks and (2) define whether this cortical area can generate fast activity patterns when isolated from other brain regions.

Materials and Methods

Brain slice preparation and maintenance

Coronal or sagittal slices, 450 μm thick, were obtained from 6- to 8-week-old male Sprague-Dawley rats (Charles River, Saint Constant, Quebec, Canada). Animals were anesthetized with isoflurane and decapitated. Their brains were quickly removed and chilled in ice-cold artificial cerebrospinal fluid (ACSF) of the following composition (mM): 124 NaCl, 2 KCl, 2 $CaCl_2$, 2 $MgSO_4$, 1.25 KH_2PO_4, 26 $NaHCO_3$, 10 D-glucose, continuously bubbled with O_2/CO_2 (95/5%) gas mixture to equilibrate at pH ~7.4. Slices were cut with a Vibratome (VT1000S; Leica, Concord, ON, Canada) and immediately transferred to an interface chamber, where they laid between warm (31–33°C) ACSF (pH ~7.4, ~305 mOsm/kg) and humidified gas (O_2/CO_2, 95/ 5%). Slices were allowed to recover for ≥1 h before beginning continuous bath-application (~2 ml/min) of 4AP (50 μM). All drugs were bath-applied; chemicals were acquired from Sigma-Aldrich Canada, Ltd. (Oakville, ON, Canada) and from Tocris Bioscience (Ellisville, MO, U.S.A.). All the procedures were carried on in compliance with the guidelines of the Canadian Council on Animal Care and the McGill Animal Care Committee to minimize the number of animals used and their suffering.

Field potential recording

Field potential recordings were performed with ACSF-filled glass pipettes (1B150F-4;World Precision Instruments, Sarasota, FL, U.S.A.; tip diameter <10 μm, resistance 5–10 MΩ) pulled with a Sutter P-97 puller (Sutter, Novato, CA, U.S.A.). Signals were fed onto an AxoClamp-2B amplifier and a CyberAmp 380 (Molecular Devices, Silicon Valley CA, U.S.A.), digitized with the Digidata 1322A (Molecular Devices) and acquired on the hard drive of a personal computer using the software CLAMPEX 8.2 (Molecular Devices). Signals acquired with the CyberAmp 380 were sampled at 10 KHz and low-passed at 2 KHz.

Data and statistical analysis

Offline analysis of duration, interval, and time-delays of epileptiform discharges was performed using the software CLAMPFIT 9 (Molecular Devices). To segregate interictal-like (hereafter termed interictal) from ictal-like (hereafter termed ictal) activity, we applied the k-means clustering algorithm with squared euclidean distances on the duration of all recorded events in order to classify them as either ictal or interictal discharges. Appropriate clustering of data was obtained with two groups, with a cutoff at 2.5 s. Therefore, all events ≥2.5 s were considered as ictal activity, whereas those lasting <2.5 s were considered as interictal events (cf. the distribution of event duration in Fig. 1C). Time-delay measurements for identification of epileptiform discharge onset region in sagittal slices were obtained by taking as temporal reference the first deflection from the baseline in expanded traces. The anterior PC was taken as time reference; therefore, positive delays indicate an anterior origin of the event while negative delays correspond to events initiated in the posterior zone. Bin

size to build the frequency distributions of time delays was 5 and 2 ms for interictal and ictal events, respectively.

To detect and to analyze HFOs, data files were exported offline with MATLAB 7.9.0 (MathWorks, Natick, MA, U.S.A.). A multiparametric algorithm was employed to identify oscillations in the high-frequency range (80–500 Hz), using routines based on standardized functions (Signal Processing Toolbox). Field potentials were analyzed from 60 s before the onset of the ictal event to 50 s after the end of the event. Recordings were then band-pass filtered in the 80–200 Hz and in the 250–500 Hz frequency range using an finite impulse response (FIR) filter; zero-phase digital filtering was used to avoid phase distortion. For each recording a 10 s artifact-free period (40–50 s before the onset of the ictal event) was selected as the reference period for signal normalization. To be considered a potential HFO candidate, oscillatory events in the 80–200 Hz and in the 250–500 Hz frequency range had to show three consecutive peaks three standard deviations (SDs) above the mean of the reference period, with a time lag between 5 and 12.5 ms between consecutive peaks for oscillations in the 80–200 Hz range and between 2 and 4 ms for events in the 250–500 Hz range. HFO events were considered for further analysis only if an oscillatory event was visible in the 80–200 Hz range and oscillations in the 250–500 Hz range were kept for analysis only if they were visible in that frequency range. Every ictal event was then divided in 1 s bins and the occurrence of HFOs was calculated for each bin. Bar graphs were then built using the number of HFO events in each bin and the average rate of HFOs was calculated using all ictal events recorded. Ictal discharges were detected using a custom-built program in MATLAB. The same field potential recordings used for HFO analysis were employed for ictal discharge analysis. Field potentials were normalized using the background mean and ictal discharges above a threshold—which was adjusted for each ictal event to match what was observed with visual analysis— were kept for analysis. The average discharge rate per bin was calculated for all ictal events. This approach allowed us to study the occurrence of HFOs during ictal discharges.

Throughout the text, n indicates the number of slices studied, unless otherwise specified. Data were compared with the Student's *t*-test or analysis of variance (ANOVA) followed by the Tukey post hoc test, or with the Fisher's exact test, as appropriate. Results were considered significantly different if $p < 0.05$. Results are expressed as mean ± standard error of the mean (SEM).

Results

4AP-Induced epileptiform activity in the rat PC

The activity generated by coronal (n = 23, Fig. 1A) or sagittal (n = 21, Fig. 1B) PC slices during 4AP application consisted of epileptiform discharges that closely resembled those observed in epileptic patients. Specifically, we could record both interictal-like and ictal-like discharges (hereafter termed interictal and ictal, respectively) (dots and solid lines in Fig. 1A,B, respectively). It should be emphasized that this pattern of epileptiform synchronization was similar to what was reported in brain slices of other limbic regions treated with 4AP (see for review Avoli & de Curtis, 2011), as well as in the insular (Sudbury & Avoli, 2007) and the cingulate (Panuccio et al., 2009) cortices. The frequency distribution

histogram of the duration of the epileptiform events recorded from sagittal slices is shown in Fig. 1C. Following k-cluster analysis of epileptiform discharges, a cutoff value of 2.5 s of duration was chosen to segregate interictal and ictal discharges (see expanded inset in Fig. 1C).

In support of the view that these field potentials originated within the PC, both types of epileptiform discharges exhibited a polarity reversal between layers I and II, when recorded in both preparations (Fig. 1, expanded boxed recordings, but see also Fig. 2A). In addition, the duration and the interval of occurrence of epileptiform events generated by coronal and sagittal brain slices were similar (see Table 1), suggesting that the minimal circuit necessary for sustaining epileptiform activity was maintained in both types of preparation (cf. Demir et al., 2001). However, sagittal slices allow for direct comparison between the epileptiform patterns generated by the anterior and the posterior PC. Therefore, we decided to pursue further electrophysiologic and pharmacologic experiments using this type of preparation. In addition, we performed most of these experiments by recording from layer II because the somata of pyramidal cells, which receive most of the inhibitory inputs, are mainly located in this layer (Haberly & Bower, 1989; Loscher & Ebert, 1996).

Figure 2A shows the electrographic details of an ictal discharge recorded from layers I and II of the anterior PC in a sagittal slice. As illustrated in Fig. 2Aa, the onset of ictal activity was usually marked by a fast spike that closely resembled that associated with each interictal discharge (Fig. 2Ad). This initial spike led to the tonic-like phase of the ictal discharge that was predominated by an oscillatory pattern at ~5 Hz (Fig. 2Ab) and was followed by clonic-like activity made of recurrent population bursts (Fig. 2Ac). A similar ictal discharge structure could be identified for the ictal events recorded from coronal slices (not illustrated).

Initiation and propagation of epileptiform activity in sagittal PC slices

The anatomic differences between the anterior and posterior subregions of the PC and the propensity of the anterior subregion for seizure initiation led us to hypothesize that epileptiform activity could be more easily induced in the anterior sector (Ekstrand et al., 2001). In particular, we wanted to test the hypothesis that synchronous epileptiform activity occurred first in the anterior region and that more posterior regions were progressively recruited later. To this aim, we analyzed the time delays of the onset of both ictal and interictal events recorded from the anterior and posterior PC (Fig. 2B). As indicated by the frequency distribution of time delays in Fig. 2B, the anterior PC appeared to drive the generation of ictal discharges. In fact, 69% of ictal events (n = 20/29 events from six slices) were first observed in the anterior PC, from where they propagated to the posterior subregion ($p < 0.001$, Fisher's exact test). Instead, interictal activity (n = 218 events from six slices) could initiate in either of the two subregions, with no preferential site of origin; each of the two subregions was the apparent site of initiation of 50% (109/218) of the interictal events.

HFOs and epileptiform activity

Next, we wanted to verify in sagittal slices whether the leading role of the anterior PC in driving the generation of ictal discharges was paralleled by differences between the two PC subregions in the generation of HFOs (80–500 Hz). Therefore, we analyzed 22 ictal events from four slices, comprising a total of 881 and 1,020 HFOs recorded from the anterior and the posterior PC, respectively. Band-pass filtering in the 250–500 Hz frequency range did not reveal the presence of any significant HFO activity at this frequency range. In contrast, both PC subregions generated HFOs at 80–200 Hz; these HFOs were similar in duration (anterior PC, 21.1 ± 8.43 msec; posterior PC, 24.7 ± 9.7 msec) occurred preferentially during ictal events and were rarely observed during the interictal periods in both PC subregions. In addition, as shown in Fig. 3, HFOs were mainly evident during the initial phase of the ictal discharge in both the anterior (Fig. 3A) and the posterior (Fig. 3B) subregions, and they often coincided with fast field potential transients (spikes) occurring during the ictal activity (see expanded time scale in Fig. 3A–B).

The number of HFOs detected during the ictal activity generated by the anterior and posterior PC was not significantly different (Fig. 4A). Moreover, group analysis showed similar patterns of HFO occurrence in the two subregions (Fig. 4B,C). An increase of HFO occurrence was observed at the initial phase of ictal events, with a peak being reached approximately 10 s after the onset. HFOs then decreased gradually over time and could no longer be detected upon return to baseline.

Role of excitatory and inhibitory neurotransmission on 4AP-induced epileptiform synchronization

It has been established that ionotropic glutamatergic receptor–mediated signaling is necessary for the generation of epileptiform activity in limbic brain areas challenged with 4AP (Avoli & de Curtis, 2011). Therefore, we first asked whether the occurrence of epileptiform discharges is contributed by ionotropic glutamatergic mechanisms in the PC as well.

As shown in Fig. 5A, blockade of NMDA receptor–mediated transmission (n = 4) by the competitive antagonist 3,3-(2-carboxypiperazine-4-yl)propyl-1-phosphonate (CPP, 10 μM) readily suppressed ictal activity but failed to affect interictal events, which had duration (0.69 ± 0.34 s) and continued to occur at an interval (3.22 ± 0.99 s) similar to what measured during control condition (duration: 0.71 ± 0.35 s; interval: 2.08 ± 0.23 s; p = 0.10; Fig. 5B). Subsequent application of the 2-amino-3-(5-methyl-3-oxo-1,2-oxazol-4-yl)propanoic acid (AMPA)/kainate receptor antagonist 6-cyano-7-nitroquinoxaline-2,3-dione (CNQX, 10 μM) disclosed the generation of slow field potentials (Fig. 5A), which were longer in duration (mean duration: 3.18 ± 0.93 s) and occurred less frequently (mean interval: 91.75 ± 24.70 s) than the interictal discharges recorded both during control condition and subsequent application of CPP (p = 0.002; Fig. 5B). These slow events were composed of an initial fast, negative-going deflection followed by a slower, positive-going component (not always detectable) and they were mostly observed in the posterior PC, where they had greater amplitude (see expanded traces in Fig. 5A, insets). Subsequent application of the $GABA_A$

receptor blocker picrotoxin (100 μM) abolished these slow interictal events (n = 3; not shown, but see Avoli & de Curtis, 2011), thus substantiating their GABAergic nature.

The results described above lead us to hypothesize that $GABA_A$ receptor signaling may play a central role in epileptiform synchronization in the PC, as it has been previously demonstrated for other structures of the limbic system (see for review Avoli & de Curtis, 2011). As illustrated in Fig. 5C, application of picrotoxin (100 μM) during perfusion with 4AP profoundly modified the interictal–ictal pattern generated by PC networks. This procedure abolished the occurrence of ictal events and unmasked a new pattern of recurrent synchronous discharges that were clustered thus appearing to be longer in duration than those generated during perfusion with 4AP only (duration in control: 0.54 ± 0.23 s; +PTX: 2.95 ± 0.64 s; n = 4; p = 0.03).

Discussion

Consistent with previous findings, we have shown here that during 4AP application the PC can generate both interictal and ictal activities that are similar to those generated by other limbic structures under the same experimental condition. Specifically, our results demonstrate that the occurrence of ictal discharges is contributed by NMDA receptor–mediated signaling and it is paralleled by the emergence of HFOs at 80–200 Hz. We have also found that interictal events necessitate fast ionotropic glutamatergic transmission mediated by AMPA/kainate receptor, and that intact $GABA_A$ receptor–mediated signaling is required for the generation of prolonged periods of epileptiform synchronization as seen during ictogenesis.

Ictal discharge pattern generated by PC networks in vitro

Full-blown seizure-like events were seldom observed and analyzed in previous in vitro brain slice studies. In our experimental conditions, recurrent ictal discharges were initiated primarily in the anterior PC. The higher propensity of the anterior subregion to generate ictal activity is not surprising since it has been reported that GABAergic inhibitory inputs are less pronounced in this area as compared to the posterior PC (Luna & Pettit, 2010). However, it should be emphasized that 31% of ictal events were first observed in the posterior PC from where they propagated to the anterior subregion. It is worth mentioning that, although not shown in the present work, preliminary findings obtained in our laboratory indicate that both the anterior and the posterior PC may act as independent generators of ictal events, since this type of epileptiform discharge is still observed in both subregions even when separated by knife-cut. Taken together, these findings suggest the existence of a functional interplay between these two areas, which may act as coupled oscillators promoting PC ictogenesis.

PC networks can generate HFOs in vitro

Our study shows for the first time the occurrence of HFOs in the PC in the 4AP in vitro model of ictogenesis. Previous studies have described oscillations in the 50–100 Hz range in the PC of awake and urethane anesthetized animals (Vanderwolf, 2000; Neville & Haberly, 2003; Beshel et al., 2007), but none have reported oscillations in higher frequency ranges (100–500 Hz) during ictal discharges. We have found here that ictal events in the anterior

and posterior regions of the PC are mainly characterized by oscillations in the 80–200 Hz range after onset, with no significant activity in the 250–500 Hz range. These results thus suggest that HFOs may reflect ictogenic processes in the 4AP model. Although the underlying neurophysiologic correlates of HFOs remain largely undefined, we are inclined to speculate that the virtual absence of oscillations in the 250–500 Hz range may indicate that PC ictogenesis in the 4AP model does not rely on principal cell synchronization, since HFOs at >200 Hz are thought to represent the synchronized activity of pyramidal neurons (Dzhala & Staley, 2004; Spampanato & Mody, 2007).

The well-known enhancing effect of 4AP on GABAergic transmission (Avoli & de Curtis, 2011) could indeed promote the occurrence of HFOs in the 80–200 Hz range, since high frequency activity in this range is known to be blocked following GABA antagonists (Nimmrich et al., 2005) and increased following the administration of GABAergic agonists (Koniaris et al., 2010). Moreover, the increased occurrence of HFOs in the 80–200 Hz range following the onset of a seizureas reported here further supports the hypothesis that GABAergic signaling plays a fundamental role in seizure initiation and generation in the PC following 4AP treatment. This conclusion has been drawn in several previous studies that were conducted in rodent brain slices of different limbic structures during application of 4AP or low-Mg^{2+} medium (reviewed by Avoli & de Curtis, 2011; see also next section).

Involvement of excitatory and inhibitory neurotransmissions in the generation of 4AP-induced epileptiform discharges

Pharmacologic manipulation of glutamatergic and GABAergic activities in sagittal PC slices evidenced some striking similarities with what is observed in other brain regions, which are part of the limbic system (cf. Avoli & de Curtis, 2011). The occurrence of 4AP-induced interictal events was not influenced by NMDA receptor antagonists, but was significantly modified when AMPA/kainate receptors were pharmacologically blocked. This manipulation also revealed the underlying presence of slow, biphasic interictal field potentials, which were mainly contributed by $GABA_A$ receptor–mediated activity.

Remarkably, NMDA receptor appeared to play a primary role in 4AP-induced ictal synchronization. However, PC slices could no longer generate ictal discharges when deprived of the GABAergic drive, and the epileptiform activity induced by 4AP treatment turned into an interictal-like pattern. The different ability of 4AP and bicuculline/ picrotoxin treatments to induce ictal activity has also been evidenced by experiments performed using the isolated guinea pig brain preparation, where 4AP promoted ictal synchronization (Carriero et al., 2010), whereas GABAergic blockers induced only large and periodic interictal spikes (de Curtis et al., 1994; Forti & Michelson, 1997; Librizzi & de Curtis, 2003). The same pattern was observed by Rigas and Castro-Alamancos (2004) in mouse PC slices treated with bicuculline. Therefore, our findings further substantiate the leading role of GABAergic signaling in driving neuronal networks toward synchronized activity, as previously described for limbic networks (Avoli & de Curtis, 2011), the insular (Sudbury & Avoli, 2007) and the cingulate (Panuccio et al., 2009) cortices, where a similar switch in discharge pattern was observed upon coperfusion of 4AP with GABA-receptor blockers.

Conclusions

We have shown here that PC networks maintained in vitro in a brain slice preparation can, in the presence of 4AP, sustain interictal and ictal discharges. Remarkably, these findings are different from those obtained in the isolated whole guinea pig brain in vitro preparation (Carriero et al., 2010). In this study, PC networks generated a stereotyped pattern of field potential oscillations at 20–60 Hz, whereas interictal and ictal events were recorded in hippocampus and entorhinal cortex but did not propagate to the PC. It is unclear whether these differences are species-related or if they reflect the different degree of connectivity present in the two preparations. However, it should be emphasized that the patterns of epileptiform discharge generated by rat PC networks are surprisingly similar (also for the pharmacological profiles) to those induced by 4AP in rodent slices of several limbic and extralimbic structures (Avoli& de Curtis, 2011).

A novel finding reported in our study relates to the presence of HFOs at 80–200 Hz during (and especially at the onset of) ictal activity. Several studies have proposed that HFOs in this frequency range reflect the activity of interneurons (see for review Avoli & de Curtis, 2011). Given the role played by GABAergic mechanisms in 4AP-induced ictogenesis, it could be hypothesized that these HFOs reflect the interaction between pyramidal and interneural network activity (Buzsáki et al., 1992; Buzsáki & Chrobak, 1995; Draguhn et al., 2000; Csicsvari et al., 1998, 1999); as HFOs in the 80–200 Hz frequency range could represent summed inhibitory postsynaptic potentials (IPSPs) in pyramidal cells as a result of high-frequency activity of interneuronal networks, firing in-phase or out-of-phase with the field oscillation (Ylinen et al., 1995). Future intracellular analysis of PC neurons recorded during 4AP application will be required to firmly establish their nature.

Acknowledgments

This study was supported by the CIHR, Grant MOP-8109, and by the Italian Health Ministry (*Ricerca Corrente* 2010 and *Progetto Giovani Ricercatori* 2008). GP is a recipient of the Savoy Foundation postdoctoral research award. We thank Ms. R. Herrington and Mr. H. Yver for helping with the data analysis.

References

Avoli M, de Curtis M. GABAergic synchronization in the limbic system and its role in the generation of epileptiform activity. Prog Neurobiol. 2011; 95:104–132. [PubMed: 21802488]

Beshel J, Kopell N, Kay LM. Olfactory bulb gamma oscillations are enhanced with task demands. J Neurosci. 2007; 27:8358–8365. [PubMed: 17670982]

Buzsáki G, Horváth Z, Urioste R, Hetke J, Wise K. High-frequency network oscillations in the hippocampus. Science. 1992; 256:1025–1027. [PubMed: 1589772]

Buzsáki G, Chrobak J. Temporal structure in spatially organized neuronal ensembles: a role for interneuronal networks. Curr Opin Neurobiol. 1995; 5:504–510. [PubMed: 7488853]

Carlsen J, De Olmos J, Heimer L. Tracing of two-neuron pathways in the olfactory system by the aid of transneuronal degeneration: projections to the amygdaloid body and hippocampal formation. J Comp Neurol. 1982; 208:196–208. [PubMed: 6181105]

Carriero G, Uva L, Gnatkovsky V, Avoli M, de Curtis M. Independent epileptiform discharge patterns in the olfactory and limbic areas of the in vitro isolated Guinea pig brain during 4-aminopyridine treatment. J Neurophysiol. 2010; 103:2728–2736. [PubMed: 20220076]

Csicsvari J, Hirase H, Czurko A, Buzsáki G. Reliability and state dependence of pyramidal cell-interneuron synapses in the hippocampus: an ensemble approach in the behaving rat. Neuron. 1998; 21:179–189. [PubMed: 9697862]

Csicsvari J, Hirase H, Czurkó A, Mamiya A, Buzsáki G. Oscillatory coupling of hippocampal pyramidal cells and interneurons in the behaving rat. J Neurosci. 1999; 19:274–287. [PubMed: 9870957]

de Curtis M, Biella G, Forti M, Panzica F. Multifocal spontaneous epileptic activity induced by restricted bicuculline ejection in the piriform cortex of the isolated guinea pig brain. J Neurophysiol. 1994; 71:2463–2476. [PubMed: 7931528]

Demir R, Haberly LB, Jackson MB. Voltage imaging of epileptiform activity in slices from rat piriform cortex: onset and propagation. J Neurophysiol. 1998; 80:2727–2742. [PubMed: 9819277]

Demir R, Haberly LB, Jackson MB. Sustained plateau activity precedes and can generate ictal-like discharges in low-Cl(−) medium in slices from rat piriform cortex. J Neurosci. 1999a; 19:10738–10746. [PubMed: 10594057]

Demir R, Haberly LB, Jackson MB. Sustained and accelerating activity at two discrete sites generate epileptiform discharges in slices of piriform cortex. J Neurosci. 1999b; 19:1294–1306. [PubMed: 9952407]

Demir R, Haberly LB, Jackson MB. Imaging epileptiform discharges in slices of piriform cortex with voltage-sensitive fluorescent dyes. Ann N Y Acad Sci. 2000; 911:404–417. [PubMed: 10911888]

Demir R, Haberly LB, Jackson MB. Epileptiform discharges with in-vivo-like features in slices of rat piriform cortex with longitudinal association fibers. J Neurophysiol. 2001; 86:2445–2460. [PubMed: 11698534]

Draguhn A, Traub RD, Bibbig A, Schmitz D. Ripple (approximately 200-Hz) oscillations in temporal structures. J Clin Neurophysiol. 2000; 17:361–376. [PubMed: 11012040]

Dzhala VI, Staley KJ. Mechanisms of fast ripples in the hippocampus. J Neurosci. 2004; 6:8896–8906.

Ebert U, Wlaz P, Loscher W. High susceptibility of the anterior and posterior piriform cortex to induction of convulsions by bicuculline. Eur J Neurosci. 2000; 12:4195–4205. [PubMed: 11122331]

Ekstrand JJ, Domroese ME, Johnson DM, Feig SL, Knodel SM, Behan M, Haberly LB. A new subdivision of anterior piriform cortex and associated deep nucleus with novel features of interest for olfaction and epilepsy. J Comp Neurol. 2001; 434:289–307. [PubMed: 11331530]

Federico P, Borg SG, Salkauskus AG, MacVicar BA. Mapping patterns of neuronal activity and seizure propagation by imaging intrinsic optical signals in the isolated whole brain of the guinea-pig. Neuroscience. 1994; 58:461–480. [PubMed: 8170533]

Forti M, Michelson HB. Novel glutamate- and GABA-independent synaptic depolarization in granule cells of guinea-pig hippocampus. J Physiol. 1997; 504:641–648. [PubMed: 9401971]

Haberly LB. Parallel-distributed processing in olfactory cortex: new insights from morphological and physiological analysis of neuronal circuitry. Chem Senses. 2001; 26:551–576. [PubMed: 11418502]

Haberly LB, Bower JM. Olfactory cortex: model circuit for study of associative memory? Trends Neurosci. 1989; 12:258–264. [PubMed: 2475938]

Hoffman WH, Haberly LB. Bursting-induced epileptiform EPSPs in slices of piriform cortex are generated by deep cells. J Neurosci. 1991; 11:2021–2031. [PubMed: 1676726]

Hoffman WH, Haberly LB. Role of synaptic excitation in the generation of bursting-induced epileptiform potentials in the endopiriform nucleus and piriform cortex. J Neurophysiol. 1993; 70:2550–2561. [PubMed: 8120598]

Hoffman WH, Haberly LB. Kindling-induced epileptiform potentials in piriform cortex slices originate in the underlying endopiriform nucleus. J Neurophysiol. 1996; 76:1430–1438. [PubMed: 8890264]

Koniaris E, Drimala P, Sotiriou E, Papatheodoropoulos C. Different effects of zolpidem and diazepam on hippocampal sharp-wave ripple activity in vitro. Neuroscience. 2010; 23:224–234.

Krettek JE, Price JL. Projections from the amygdaloid complex and adjacent olfactory structures to the entorhinal cortex and to the subiculum in the rat and cat. J Comp Neurol. 1977; 172:723–752. [PubMed: 838896]

Krettek JE, Price JL. Amygdaloid projections to subcortical structures within the basal forebrain and brainstem in the rat and cat. J Comp Neurol. 1978; 178:225–254. [PubMed: 627625]

Laufs H, Richardson MP, Salek-Haddadi A, Vollmar C, Duncan JS, Gale K, Lemieux L, Löscher W, Koepp MJ. Converging PET and fMRI evidence for a common area involved in human focal epilepsies. Neurology. 2011; 77:904–910. [PubMed: 21849655]

Libri V, Constanti A, Zibetti M, Nisticó S. Effects of felbamate on muscarinic and metabotropic-glutamate agonist-mediated responses and magnesium-free or 4-aminopyridine-induced epileptiform activity in guinea pig olfactory cortex neurons in vitro. J Pharmacol Exp Ther. 1996; 277:1759–1769. [PubMed: 8667248]

Librizzi L, de Curtis M. Epileptiform ictal discharges are prevented by periodic interictal spiking in the olfactory cortex. Ann Neurol. 2003; 53:382–389. [PubMed: 12601706]

Loscher W, Ebert U. The role of the piriform cortex in kindling. Prog Neurobiol. 1996; 50:427–481. [PubMed: 9015822]

Luna VM, Pettit DL. Asymmetric rostro-caudal inhibition in the primary olfactory cortex. Nat Neurosci. 2010; 13:533–535. [PubMed: 20348915]

Luskin MB, Price JL. The laminar distribution of intracortical fibers originating in the olfactory cortex of the rat. J Comp Neurol. 1983; 216:292–302. [PubMed: 6863605]

Mathern, GW., Babb, TL., Armstrong, DL. Hippocampal sclerosis. In: Engel, J., Pedley, TA., editors. Epilepsy: A Comprehensive Textbook. Lippincott-Raven; Philadelphia, PA: 1997. p. 133-155.

McIntyre DC, Plant JR, Kelly ME. Dorsal hippocampal kindling produces long-lasting changes in the origin of spontaneous discharges in the piriform versus perirhinal cortex in vitro. Epilepsy Res. 2000; 39:191–200. [PubMed: 10771245]

Neville KR, Haberly LB. Beta and gamma oscillations in the olfactory system of the urethane-anesthetized rat. J Neurophysiol. 2003; 90:3921–3930. [PubMed: 12917385]

Nimmrich V, Maier N, Schmitz D, Draguhn A. Induced sharp wave-ripple complexes in the absence of synaptic inhibition in mouse hippocampal slices. J Physiol. 2005; 563:663–670. [PubMed: 15661820]

Panuccio G, Curia G, Colosimo A, Cruccu G, Avoli M. Epileptiform synchronization in the cingulate cortex. Epilepsia. 2009; 50:521–536. [PubMed: 19178556]

Piredda S, Gale K. A crucial epileptogenic site in the deep prepiriform cortex. Nature. 1985; 317:623–625. [PubMed: 4058572]

Price JL. An autoradiographic study of complementary laminar patterns of termination of afferent fibers to the olfactory cortex. J Comp Neurol. 1973; 150:87–108. [PubMed: 4722147]

Rigas P, Castro-Alamancos MA. Leading role of the piriform cortex over the neocortex in the generation of spontaneous interictal spikes during block of GABA(A) receptors. Neuroscience. 2004; 124:953–961. [PubMed: 15026135]

Russchen FT. Amygdalopetal projections in the cat. I. Cortical afferent connections. A study with retrograde and anterograde tracing techniques. J Comp Neurol. 1982; 206:159–179. [PubMed: 7085926]

Schwabe K, Ebert U, Loscher W. Bilateral lesions of the central but not anterior or posterior parts of the piriform cortex retard amygdala kindling in rats. Neuroscience. 2000; 101:513–521. [PubMed: 11113300]

Shipley MT, Ennis M. Functional organization of olfactory system. J Neurobiol. 1996; 30:123–176. [PubMed: 8727988]

Spampanato J, Mody I. Spike timing of lacunosom-moleculare targeting interneurons and CA3 pyramidal cells during high-frequency network oscillations in vitro. J Neurophysiol. 2007; 98:96–104. [PubMed: 17475718]

Sudbury JR, Avoli M. Epileptiform synchronization in the rat insular and perirhinal cortices in vitro. Eur J Neurosci. 2007; 26:3571–3582. [PubMed: 18052975]

Uva L, Librizzi L, Wendling F, de Curtis M. Propagation dynamics of epileptiform activity acutely induced by bicuculline in the hippocampal-parahippocampal region of the isolated Guinea pig brain. Epilepsia. 2005; 46:1914–1925. [PubMed: 16393157]

Vanderwolf CH. What is the significance of gamma activity in the piriform cortex? Brain Res. 2000; 877:125–133. [PubMed: 10986324]

Veening JG. Cortical afferents of the amygdaloid complex in the rat: an HRP study. Neurosci Lett. 1978; 8:191–195. [PubMed: 19605157]

Wakefield C. The topographical organization and laminar origin of some cortico-amygdaloid connections. Neurosci Lett. 1980; 20:21–24. [PubMed: 6302603]

Ylinen A, Bragin A, Nádasdy Z, Jandó G, Szabó I, Sik A, Buzsáki G. Sharp wave-associated high-frequency oscillation (200 Hz) in the intact hippocampus: network and intracellular mechanisms. J Neurosci. 1995; 15:30–46. [PubMed: 7823136]

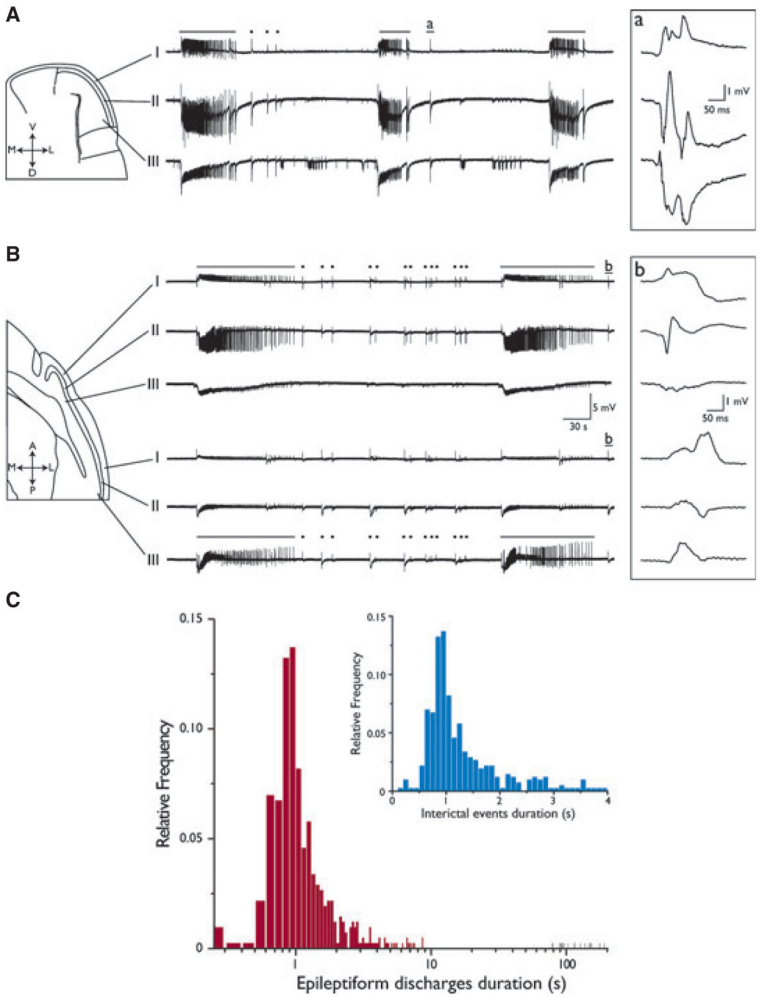

Figure 1.

4AP-Induced epileptiform activity in PC coronal and sagittal slices. Field potential recordings from a coronal (**A**) and sagittal (**B**) PC slice. Electrodes were positioned in layers I, II, and III, as depicted in the slice schematics. Continuous superfusion with 4AP induced the generation of both ictal (solid lines) and interictal (dots) events. Boxed traces represent the interictal events indicated by insets a and b, shown at a faster time scale. Note the reversion of signal polarity between superficial and deep layers. (**C**) Frequency distribution histograms of event duration plotted on a log scale, showing a segregation of interictal-like and ictal-like events. As further emphasized in the inset (expanded linear scale), the latter were defined as events lasting longer than 2.5 s.

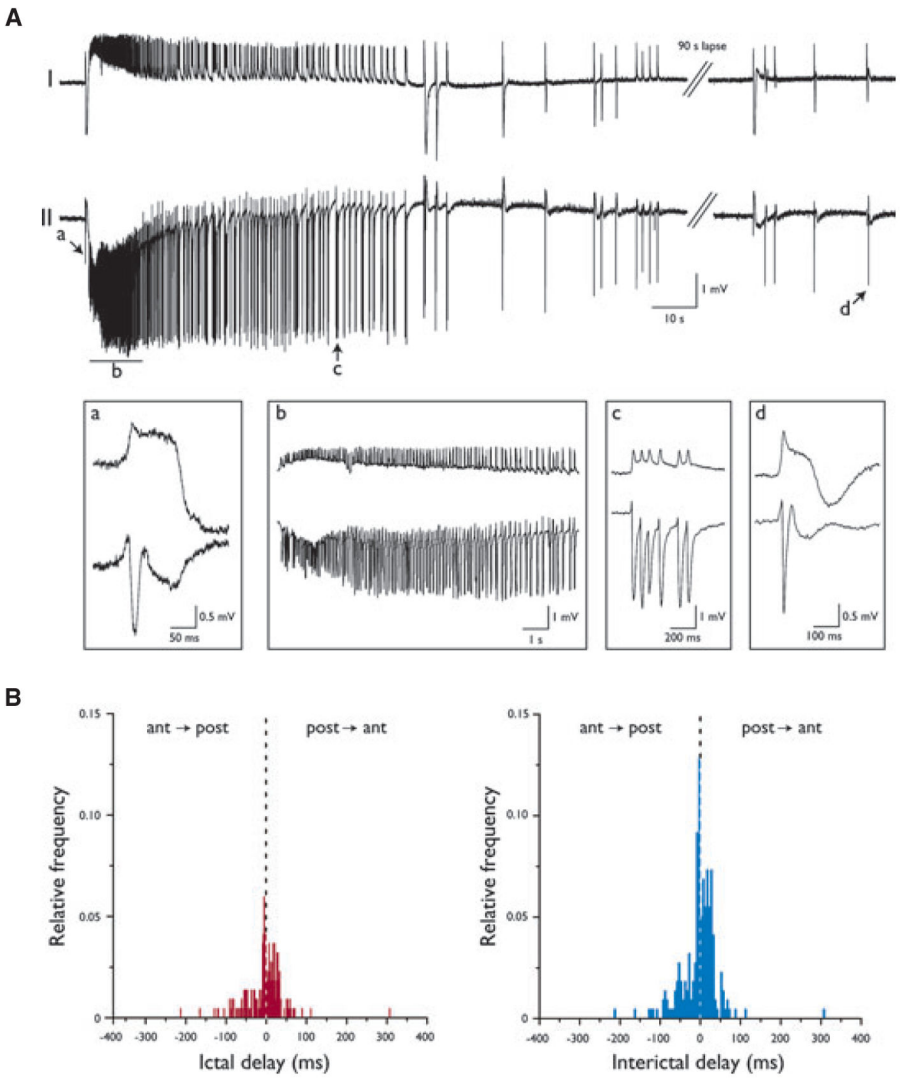

Figure 2.

4AP-Induced epileptiform discharges in sagittal PC slices. (**A**) Recording obtained from layers I and II of the anterior PC showing the generation of an ictal discharge followed by the occurrence of interictal events. The onset of ictal activity is preceded by a fast field event (expanded in **a**) resembling an interictal discharge (**d**). The ictal event is characterized by the initial manifestation of tonic activity (**b**), which gradually slows down and is replaced by clonic discharges made of population bursts (**c**). (**B**) Frequency distributions of time delays of epileptiform events. The anterior PC appears to drive the generation of ictal activity, whereas interictal events are generated equally by both the anterior and the posterior subregions.

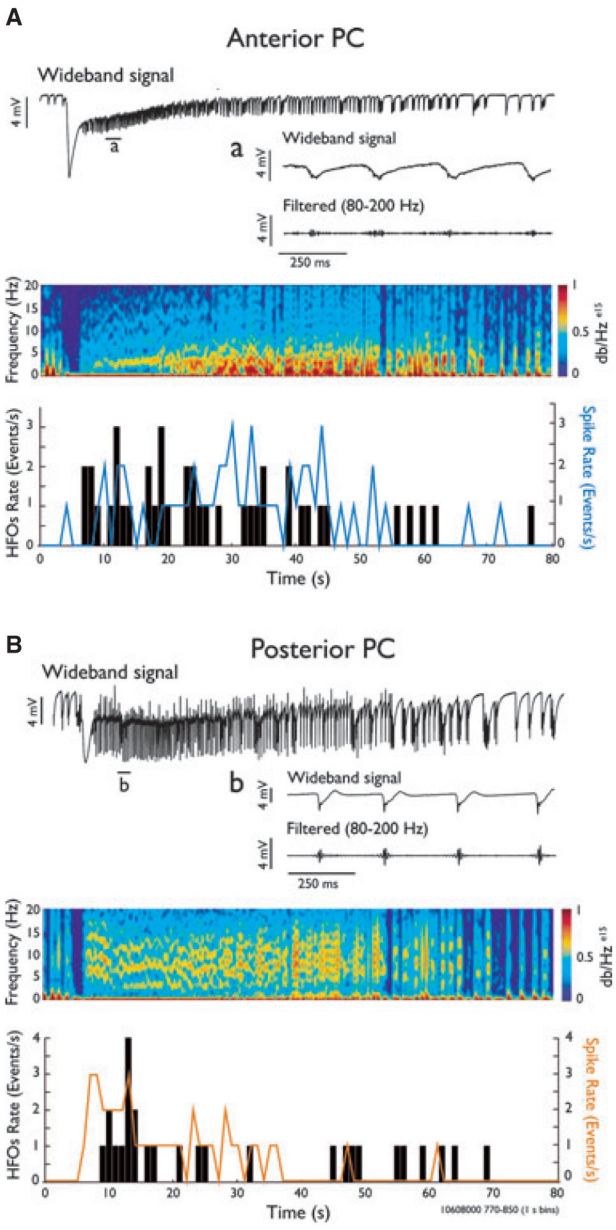

Figure 3.

High frequency oscillation in the 80–200 Hz range is associated with ictal events. Recordings from a sagittal brain slice with corresponding spectral analyses showing an ictal discharge in the anterior (**A**) and posterior (**B**) regions. Wideband and filtered traces (80–200 Hz) showing high-frequency activity during a 1 s time period are shown in **a** and **b**. Time histograms (1 s bins) indicate the HFO occurrence (black bars, 1 s bins) and the frequency of spikes occurring during ictal activity (solid lines) for the events shown in **A** and **B**.

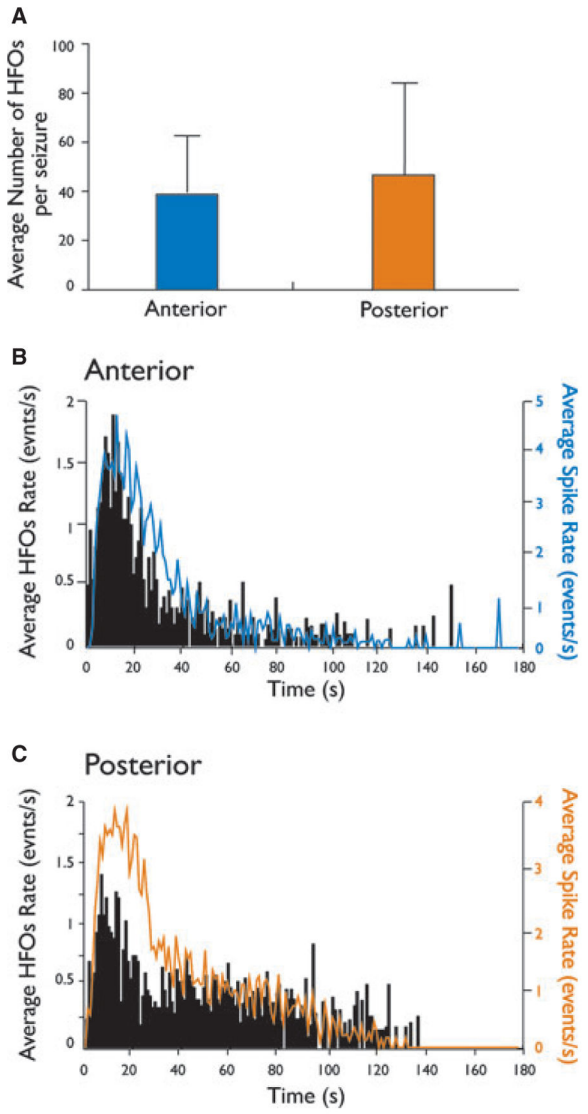

Figure 4.

Time distribution patterns of high-frequency activity during ictal discharges. (**A**) Bar graph showing the average number of events in the 80–200 Hz range during ictal discharges in the anterior and posterior regions of the piriform cortex in four slices, 22 ictal events. (**B** and **C**) Bar histograms showing the average rates of HFO events and the frequency of spikes occurring during ictal activity for the anterior and posterior regions of the PC. In both subregions, high-frequency activity was observed during the initial phase of ictal discharges.

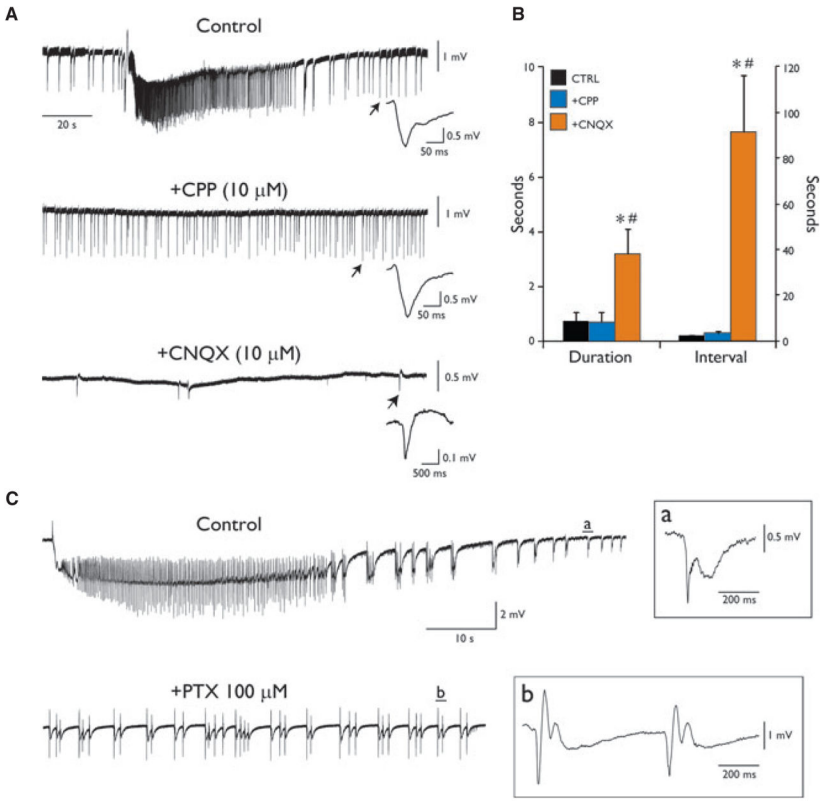

Figure 5.

Pharmacologic profile of 4AP-induced epileptiform activities in the PC. (**A**) Pharmacologic blockade of the NMDA receptor by CPP abolishes ictal activity without affecting the generation of interictal events. Subsequent application of the AMPA/kainate antagonist CNQX discloses the occurrence of slow biphasic field potentials. On the right of each recording is shown, at a faster time scale, the event indicated by the arrows in the corresponding traces. Note the positive-going component of the event recorded in the absence of ionotropic glutamatergic signaling (all expanded interictal-like events are truncated before recovery to baseline to emphasize the emergence of the positive-going component during concomitant blockade of NMDA and AMPA/kainate receptors). (**B**) Plots of mean duration and interval of occurrence of interictal discharges recorded during control condition and during subsequent blockade of ionotropic glutamatergic receptors. *Indicates significance against Control; #Indicates significance against +CPP. (**C**) Blockade of $GABA_A$ receptor abolishes ictal activity and discloses the generation of recurrent interictal discharges.

Table 1

Duration and interval of occurrence of epileptiform discharges in coronal and sagittal PC slices

	Sagittal slices (n = 21)	Coronal slices (n = 23)
Ictal discharge		
Duration (s)	92.0 ± 5.3	98.4 ± 7.4
Interval (min)	4.9 ± 0.4	4.6 ± 0.4
Interictal event		
Duration (s)	0.9 ± 0.2	1.4 ± 0.4
Interval (s)	28.6 ± 15.6	40.2 ± 11.3

No statistical differences were found when comparing the activities recorded from the two preparations.